arXiv:1301.6970v1 [quant-ph] 29 Jan 2013

Non-classicality of molecular vibrations activating electronic dynamics at room temperature

Edward J. O'Reilly[1] and Alexandra Olaya-Castro[1, a)]
Department of Physics and Astronomy, University College London, Gower Street, London, WC1E 6BT United Kingdom.

Advancing the debate on the possible advantages of quantum effects in biomolecular systems requires illustrations of biomolecular prototypes that can exhibit and use non-classical phenomena to aid performance. Here we investigate non-classical fluctuations in molecular dimers present in photosynthetic light-harvesting antennae. We show that exciton-vibrational resonances enable non-classical occupation fluctuations of the driven collective high-energy vibration at room temperature. This phenomenon is a manifestation of strong modulation of low-phonon occupation levels through the transient formation of hybrid exciton-vibration states. For the prototype considered, direct quantitative relations seem to hold between non-classicality and optimal exciton population transfer.

The experimental investigation of quantum effects in photosynthetic energy transfer[1–5] has inspired exciting research towards asserting the relevance of non-classical behaviour in the biological function of the molecular components of living organisms. Theoretical works have made emphasis on the quantumness exhibited by electronic degrees of freedom[6] and on the key role of environmental fluctuations[7,8]. In order to understand the full range of possible non-classical phenomena present during room-temperature dynamics of electronic excitations in light-harvesting antennae it is important to expand the analysis to the molecular motions that play a fundamental role in driving exciton transport[9]. Research in this direction is timely given that experiments[10,11] and theoretical works[12–18] are highlighting the importance of concerted electronic and vibrational dynamics in energy transfer. Moreover, recent experimental techniques able to manipulate vibrational states[19,20] and probe their quantum properties may indeed provide experimental access to the non-classicality of vibrational modes in biomolecular systems. Here we consider a prototype molecular dimer with an structured exciton-phonon interaction and investigate non-classical behaviour of molecular vibrations that steer energy dynamics and exciton coherences in this molecular unit. While previous studies have considered coherent exciton-vibration dynamics in molecular dimers[14,17,21], it is unclear how this deviates from classical (wave-like) coherent behaviour and if so whether there are quantitative relationships between non-classicality and effective energy transfer.

The prototype of interest consists of two chromophores coupled by weak electronic interactions and subject to the influence of both a low-energy thermal background and a discrete high-frequency intramolecular vibration. The key aspect of this molecular vibration is that its energy matches closely the exciton gap but it is much larger than the thermal energy scale. Dimers of this type naturally occur in several light-harvesting proteins[12,22] and are of particular interest as they represent systems where, although counter-intuitive, exciton coherence beating has been probed[23]. Insights into the importance of resonances between exciton energy mismatch and vibrational frequencies for efficient energy transfer can be gained from Förster theory[24]. However, the wider implications of such resonances for optimal spatio-temporal distribution of energy[16,25], for manipulation of exciton coherence[13,14,16] and for non-adiabatic excitation dynamics[18] have only started to be clarified. An issue that remains to be tackled, is the extent to which such resonances can expose the non-classical features of the molecular motions activating transport. In the dimer investigated here, commensurate energies of exciton gap and discrete vibrations imply that after input of exciton population, effective energy distribution proceeds by driving the collective relative displacement mode out of thermal equilibrium towards a non-classical state. Non-classicality of the state of this relative motion is unambiguously indicated by sub-Poissonian occupation statistics[26] or alternatively by strong modulation of low-phonon occupations[27] and is a manifestation of transient collective coherent behaviour between excitons and vibrations. Low-energy thermal fluctuations stabilize energy distribution to the lowest exciton state before destroying non-classicality of the collective mode assisting the process. Meanwhile, coherent interaction between electronic degrees of freedom and such a mode manifests itself in the beating of excitonic coherences with frequency components that vary depending on the coupling to the thermal bath. When time-averaging over a relevant time scale, we find direct quantitative relations between population transfer and the degree of non-classicality as indicated by the average of negative values of the Mandel $Q-$parameter[26]. This relationship holds even when the electronic system is initialized in a statistical mixture of exciton states. Hence, efficient photosynthetic energy transport could take advantage of non-classicality.

The field of quantum optics has developed a solid framework to quantify the non-classicality of bosonic fields[28]. It therefore provides useful conceptual and quantitative tools to investigate non-classicality of the

---

[a)] Electronic mail: a.olaya@ucl.ac.uk

harmonic vibrational degrees of freedom of interest in this work. From the perspective of quantum optics, non-classicality arises if the state of the system of interest cannot be expressed as a statistical mixture of coherent states defining a valid probability measure, this then leads to non-positive or highly singular values of the Glauber-Sudarshan P-function or the Wigner function[29]. However, experimental characterization of these distributions is not always a straightforward task. Alternatively, it is of interest to investigate signatures of non-classicality. For a single-mode field, a sub-Poissonian occupation number distribution quantified by the Mandel's $Q-$parameter[26] is a signature of deviations from classical behaviour. The Mandel $Q-$parameter characterizes the departure of the occupation number distribution $P(n)$ from Poissonian statistics through the inequality

$$Q = \frac{\langle \hat{n}^2 \rangle - \langle \hat{n} \rangle^2}{\langle \hat{n} \rangle} - 1 < 0 \tag{1}$$

where $\langle \hat{n} \rangle$ and $\langle \hat{n}^2 \rangle$ denote the first and second moments of the bosonic number operator $\hat{n}$ respectively. Vanishing Q indicates Poissonian number statistics where the mean of $\hat{n}$ equals its variance (such is the case of a coherent state of light). For a chaotic thermal state one finds that $Q = \langle \hat{n} \rangle > 0$ indicating that particles are 'bunched'. The departure from classical (wave-like) behaviour is characterised by $Q < 0$ or particle number distributions where the variance is less than the mean, as is the case for Fock states. The occupation fluctuations associated with a sub-Poissonian distribution originate from the quantized nature of the field and cannot be described in terms of an underlying *classical* stochastic process. A criteria that directly connects non-classical occupation fluctuations and the negativity of a quasiprobability distribution is an inequality indicating modulation of nearest number occupations[27]. In this work we use the above framework to quantify non-classicality of the undamped vibrational modes supporting exciton transport in the molecular dimer of interest. We consider each chromophore with an excited electronic state of energy ε_i strongly coupled to a quantized vibrational mode of high-frequency ($\omega_{\mathrm{vib}} > K_B T$) described by the bare Hamiltonians $H_{\mathrm{el}} = \sum_{i=1,2} \varepsilon_i \sigma_i^+ \sigma_i^-$ and $H_{\mathrm{vib}} = \omega_{\mathrm{vib}}(b_1^\dagger b_1 + b_2^\dagger b_2)$ respectively. Inter-chromophore coupling is generated by dipole-dipole interactions of the form $H_{\text{d-d}} = V(\sigma_1^+ \sigma_2^- + \sigma_2^+ \sigma_1^-)$. The electronic excited states interact with their local vibrational environments with strength g, linearly displacing the corresponding mode coordinate, $H_{\text{el-vib}} = g \sum_{i=1,2} \sigma_i^+ \sigma_i^- (b_i^\dagger + b_i)$. In the above $b_i^\dagger(b_i)$ creates (annihilates) a phonon of the vibrational mode of chromophore i while $\sigma_i^\pm$ creates or destroys an electronic excitation at site i. The eigenstates $|X\rangle$ and $|Y\rangle$ of $H_{\mathrm{el}} + H_{\text{d-d}}$ denote exciton states with energy splitting given by $\Delta E = \sqrt{(\varepsilon_1 - \varepsilon_2)^2 + 4V^2}$. Transformation into collective mode coordinates shows that only the mode corresponding to the relative displacement of the modes with the bosonic operators $b^{(\dagger)} = (b_1^{(\dagger)} - b_2^{(\dagger)})/\sqrt{2}$, couples to the excitonic system. The centre of mass mode decouples from the electronic degrees of freedom. The occupation of the relative displacement mode of frequency ω_{vib} is denoted by n and the non-classical properties of such mode is the subject of interest in this article.

Our prototype system corresponds to the central dimer of the phycoerythrin 545 (PE545) antennae found in cryptophyte marine algae[30]. Exciton coherence beating involving this dimer has been probed[4] and a structured spectral density has been phenomenologically determined via linear spectroscopy[31]. The electronic parameters for the dimer taken from reference[31] are $\varepsilon_1 = 19574\mathrm{cm}^{-1}$, $\varepsilon_2 = 18532\mathrm{cm}^{-1}$ and $V = 92.2\mathrm{cm}^{-1}$. The intramolecular mode that is separated from the set of vibrational degrees of freedom has frequency $\omega_{\mathrm{vib}} = 1111\mathrm{cm}^{-1}$ being quasi-resonant with the exciton energy splitting $\Delta E = 1058.2\mathrm{cm}^{-1}$. The coupling strength of each chromophore to the this mode is $g = \omega_{\mathrm{vib}}\sqrt{0.0578} = 267.1\mathrm{cm}^{-1}$ obtained from[30,31], and the thermal energy scale at room temperature is $k_{\mathrm{B}}T \approx 200\mathrm{cm}^{-1}$. We consider the influence of the low energy thermal fluctuations via a thermal bath H_B described by a continuous distribution of harmonic modes, each linearly and independently coupled to the excited electronic states H_{el} with coupling strength characterised by a Drude spectral density $J(\omega) = (\lambda \Omega_c \omega/\pi)/(\omega^2 + {\Omega_c}^2)^2$ with reorganization energy $\lambda = 110\mathrm{cm}^{-1}$ and cut-off frequency $\Omega_c = 100\mathrm{cm}^{-1}$[32], hence the strength of the system-bath interaction is parametrized by $\sqrt{\lambda \Omega_c}$[33]. Since $J(\omega_{\mathrm{vib}}) \ll g^2$, this does not over-account for the influence of the resonant mode on the electronic system. Importantly, although the electronic coupling V is the smallest energy scale in the prototype dimer, the exciton dynamics and phonon fluctuations here investigated will not be properly described by Förster theory. In order to accurately account for the effects of the thermal bath we have extended the hierarchical expansion of the dynamics[34–36] to explicitly include the quantum interactions between electronic excitations and the selected mode. This approach allows us to account accurately for the effects of the low-energy thermal bath. In calculating dynamics we consider an initial state, in which the upper energy exciton eigenstate is rapidly excited while both high-energy quantized vibrations and low-energy thermal modes are initially in thermal equilibrium at room temperature. Truncating the quantized modes at an occupation Fock level $M = 6$ adequately describes both reduced dynamics of the collective quantized mode and the electronic dynamics. A description of the numerical methodology can be found in the appendix.

Hamiltonian dynamics and non-classicality.- We first illustrate the quantum coherent dynamics of excitation when coupled to the undamped quasiresonant high-energy vibrational modes in the absence of the low-energy thermal bath. This allows us to identify relevant time scales in the evolution of a state with no initial excitonic superpositions: $\rho(t_0) = |X\rangle \langle X| \otimes \varrho_{\mathrm{vib}}^{\mathrm{th}}$ which written in the basis of exciton-vibration states of the form $|X,n\rangle$ becomes $\rho(t_0) = \sum_n P_{th}(n)\,|X,n\rangle\,\langle X,n|$. Here n denotes the phonon occupation number of the collective mode while $P_{th}(n)$ denotes the thermal occupation of such level. We investigate the population of the lowest excitonic state $\rho_{YY}(t) = \sum_n \langle Y,n|\rho(t)|Y,n\rangle$, the absolute value of the coherence $\rho_{X0-Y0}(t) = \langle X,0|\rho(t)|Y,0\rangle$ which denotes the inter-exciton coherence in the ground-state of the collective vibrational mode, and the non-classicality given by negative values of $Q(t)$. Hamiltonian evolution generates coherent transitions from states $|X,n\rangle$ to $|Y,n+1\rangle$ (see Figure 1(a)) with a rate f that depends on the exciton delocalization ($|V|/\Delta\epsilon$), the coupling to the mode g, and the phonon occupation n i.e. $f \simeq g(2|V|/\Delta\varepsilon)\sqrt{(n+1)/2}$. Since $\omega_{\rm vib} \gg K_{\rm B}T$ the ground state of the effective mode is largely populated, such that the Hamiltonian evolution of the initial state is largely dominated by the evolution of the state $|X,0\rangle$. This implies that the energetically close exciton-vibration state $|Y,1\rangle$ becomes coherently populated at a rate $f \simeq g(2|V|/\Delta\epsilon)$, leading to the oscillatory pattern observed in the probability of occupation $\rho_{YY}(t)$ as illustrated in Figure 1 (b). The low-frequency oscillations of the dynamics of $\rho_{YY}(t)$ cannot be assigned to the exciton or the vibrational degrees of freedom alone as expected from quantum-coherent evolution of the exciton-plus-effective mode system. For instance, if the mode occupation is restricted to at most $n = 1$, the period of the amplitude of $\rho_{YY}(t)$ is given approximately by the inverse of $(1/2)(\sqrt{(\Delta E-\alpha)^2+(2g^2 4V^2/\alpha\Delta E)}-(\Delta E+\alpha))$ with $\alpha^2 = 2g^2+\omega_{\rm vib}^2$ and $(2g^2 4V^2/\alpha^2\Delta E^2) \ll 1$. Coherent exciton population transfer is then accompanied by coherent dynamics of the inter-exciton coherence $|\rho_{X0-Y0}(t)|$ with the main amplitude modulated by the same low-frequency oscillations of $\rho_{YY}(t)$ and a superimposed fast oscillatory component of frequency close to $\omega_{\rm vib}$ as can be seen in Figure 1 (b). This fast driving component arises from local oscillatory displacements: when $V \simeq 0$ the time evolution of each local mode is determined by the displacement operator with amplitude $\alpha(t) = 2g(1-\exp(-i\omega_{\rm vib}t))/\omega_{\rm vib}$[37]. As the state $|Y,1\rangle\langle Y,1|$ is coherently populated, the collective quantized mode is driven out of equilibrium towards a non-classical state in which selective occupation of the first vibrational level takes place. This manifests itself in sub-Poissonian phonon statistics as indicated by negative values of $Q(t)$ shown in Figure 1(c). Similar phenomena have been described in the context of electron transport in a nanoelectromechanical system[38,39]. Importantly, such sub-Poissonian statistics arises only when the electronic interaction is finite. For comparison, Figure 1(d) shows that if $V = 0$, a local excitation drives the mode towards a classical thermal displaced state with super-Poissonian statistics ($Q(t) > 0$). In short, non-classicality of the relative displacement mode quasiresonant with the excitonic transition arises through the formation of exciton-vibration states.

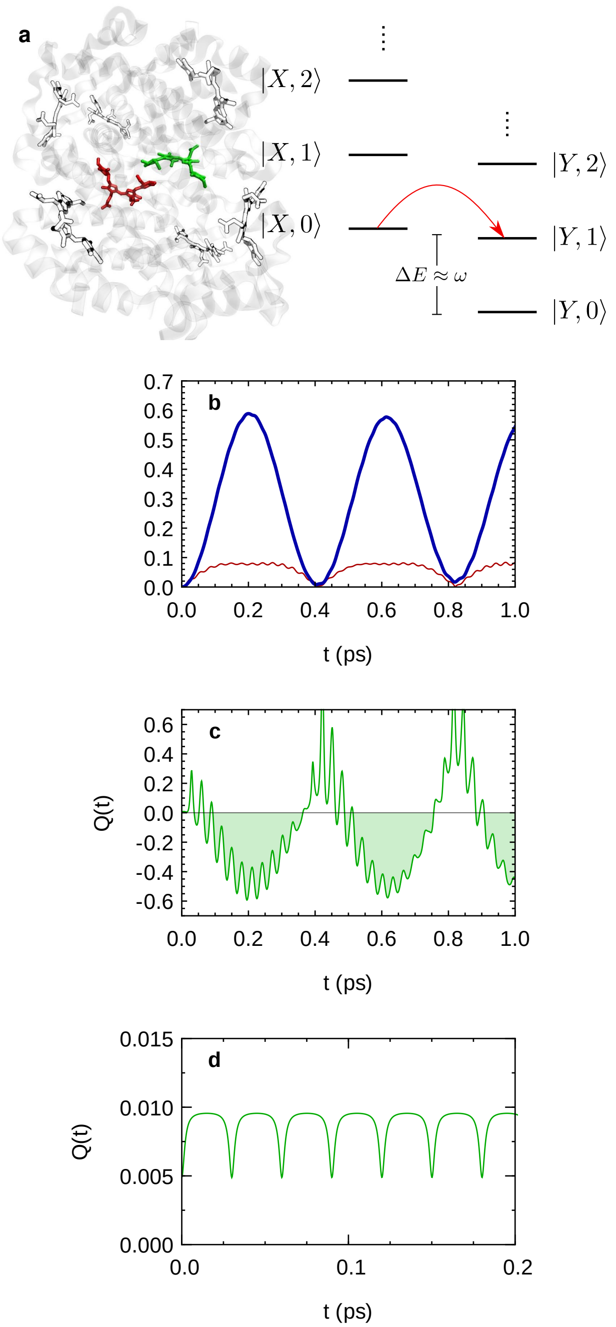

FIG. 1. **a**, Representation of the pigments and protein environment of the PE545 complex (Protein Data Bank ID code `1XG0`[30]). The central dimer is highlighted. Also shown are the energy levels of the exciton-vibration states used to describe energy transfer $|X,n\rangle$. **b**, Coherent dynamics of the exciton-vibration dimer. Oscillatory population of the lowest exciton population $\rho_{YY}(t)$ (thick blue curve) is accompanied by oscillations of the inter-exciton coherence in the ground-state of the vibrational mode $|\rho_{X0-Y0}(t)|$ (thin red curve). **c**, Mandel Q-parameter of the vibrational mode for biological electronic coupling and **d** for zero electronic coupling.

Energy and coherence dynamics - Interplay between vibration-activated dynamics and thermal fluctuations leads to two distinct regimes of energy transport. For our consideration of weak electronic coupling, the coherent transport regime is determined approximately by $\sqrt{\lambda\Omega_c} \leq 2g|V|/\Delta\epsilon$. Here population of the low-lying exciton state is dominated by coherent transitions between exciton-vibration states and the rapid short-time growth of $\rho_{YY}(t)$ in this regime can be traced back to coherent transfer of population from $|X,0\rangle\langle X,0|$ to $|Y,1\rangle\langle Y,1|$. At longer time scales thermal fluctuations induce incoherent transitions from $|X,0\rangle\langle X,0|$ to $|Y,0\rangle\langle Y,0|$ with a rate proportional to $\sqrt{\lambda\Omega_c}$, thereby stabilizing population of $|Y,1\rangle\langle Y,1|$ to a particular value (see Figure 2(a)). In contrast, for $\sqrt{\lambda\Omega_c} > 2g|V|/\Delta\epsilon$ population transfer to $\rho_{YY}(t)$ is incoherent although the dynamics is still accompanied by generation and coherent evolution of excitonic coherences (see Figures 2(g) and 2(h)). In this incoherent transport regime $\rho_{YY}(t)$ has a slow but continuous rise reflecting the fact that the incoherent transitions from $|X,0\rangle\langle X,0|$ to $|Y,0\rangle\langle Y,0|$ now contribute significantly to the transport. However, transfer to $\rho_{YY}(t)$ is always more efficient with the quasiresonant mode than in the situations where only thermal-bath induced transitions are considered (see dashed lines in Figures 2(d) and 2(g)). The underlying reason is that the system is transiently evolving towards a thermal configuration of exciton-vibration states. Hence, in both regimes excitation transfer to the lowest exciton state is achieved by transiently sharing energy with the relative displacement mode. The transition from coherent to incoherent exciton population dynamics is also marked by the onset of energy dissipation of the exciton-vibration system as shown in figures 2(c),2(f) and 2(i). While population transfer is coherent, energy dissipation into the thermal bath is prevented (Fig. 2(c) and 2(f)).

The beating patterns of the coherence $\rho_{X0-Y0}(t)$ reveals the structured nature of the exciton-phonon interaction and witnesses whether there is coherent exciton-vibration evolution. Because of this the frequency components of such oscillatory dynamics vary depending of the coupling to the thermal bath as can be seen in Figures 2(b), (e) and (h) . In the coherent regime $\rho_{X0-Y0}(t)$ follow exciton populations with the main amplitude modulated by the same relevant energy difference between exciton-vibration states (see Figures 2(b) and (e)). In contrast, in the regime of incoherent transport the short-time oscillations of $\rho_{X0-Y0}(t)$ (between $t = 0$ and $t = 0.1$ps) arise from electronic correlations due to bath-induced renormalization of the electronic Hamiltonian[40] and as such, the frequency of these short-time oscillations correspond to transitions of renormalized excitons. As the main amplitude is damped, this exciton coherence retains the superimposed driving at a frequency $\omega_{\rm vib}$. The dynamical features presented in Figures 2(g) and 2(h) confirm previous findings based on perturbative calculations[16] and agrees with the time-scales of the exciton coherence beating reported in the two-dimensional spectroscopy of cryptophyte algae[23].

Non-classicality - Interaction with a large thermal environment leads to the emergence of classicality. Indeed, as the coupling of the electronic degrees of freedom to the thermal background is increased, the maximum non-classicality of the collective mode as indicated by the most negative value of $Q(t)$ is reduced. However, the time interval for which the mode remains in a non-classical state is not a monotonic function of λ. For moderate values of λ, the relative displacement mode spends longer periods in states with non-classical fluctuations i.e. periods for which $Q(t) < 0$ as seen in Figures 3(a)-(b). Hence relatively medium coupling to a thermal background assists selective population of state $|Y,1\rangle$ thereby stabilizing non-classicality at a particular level. An important feature of the results presented in Figures 3(a)-3(c) is therefore that non-classical features surviving the picosecond time scale are present across the whole range of thermal bath couplings. This is consistent with a slow decay of the exciton-vibration coherence $\rho_{X0,Y1}$ (not shown). Interestingly, the non-classical properties of the collective mode resemble non-classicality of thermal states (completely incoherent states) that are excited by a single quanta[41]. The non-classical properties predicted by $Q(t)$ also agree with the non-classicality predicted by a parameter proposed by Klyshko[27] as is described in appendix B.

Non-classicality is witnessed by exciton population dynamics. In order to illustrate this, we now investigate quantitative relations between non-classicality and energy transport by considering relevant integrated averages in the time scale of coherent exciton-vibration dynamics denoted by τ. For the parameters chosen, this time scale is about half a picosecond and corresponds to the time in which excitation energy would be distributed away to other chromophores[16]. The time integrated averages over τ are defined as: $\langle F[\rho(t)]\rangle_\tau = \frac{1}{\tau}\int_0^\tau {\rm d}t\, F[\rho(t)]$, where $F[\rho(t)]$ corresponds to the exciton population $\rho_{YY}(t)$ and the non-classicality of the collective quantized mode through periods of sub-Poissonian statistics $Q(t)\Theta[-Q(t)]$ as functions of the coupling to the bath λ. As shown in Figure 4 the average exciton population and non-classicality follow a similar non-monotonic trend as a function of the coupling to the thermal bath, indicating a direct quantitative relation between efficient energy transfer in the time scale τ and the degree of non-classicality. The appearance of maximal point in the average non-classicality as a function of the system-bath coupling indicates that the average quantum response of the relative displacement mode to the impulsive electronic excitation, is optimal for a small amount of thermal noise.

The above results indicate that the degree of delocalization of the initial exciton state is key to enabling non-classical fluctuations of the collective quantized vibration. This suggests that statistical mixtures of excitons with finite purity can still trigger such non-classical response. To illustrate this we now consider mixed initial states of the form $\rho(t_0) = \varrho_{\rm ex} \otimes \varrho_{\rm vib}^{\rm th}$ where $\varrho_{\rm ex} =$

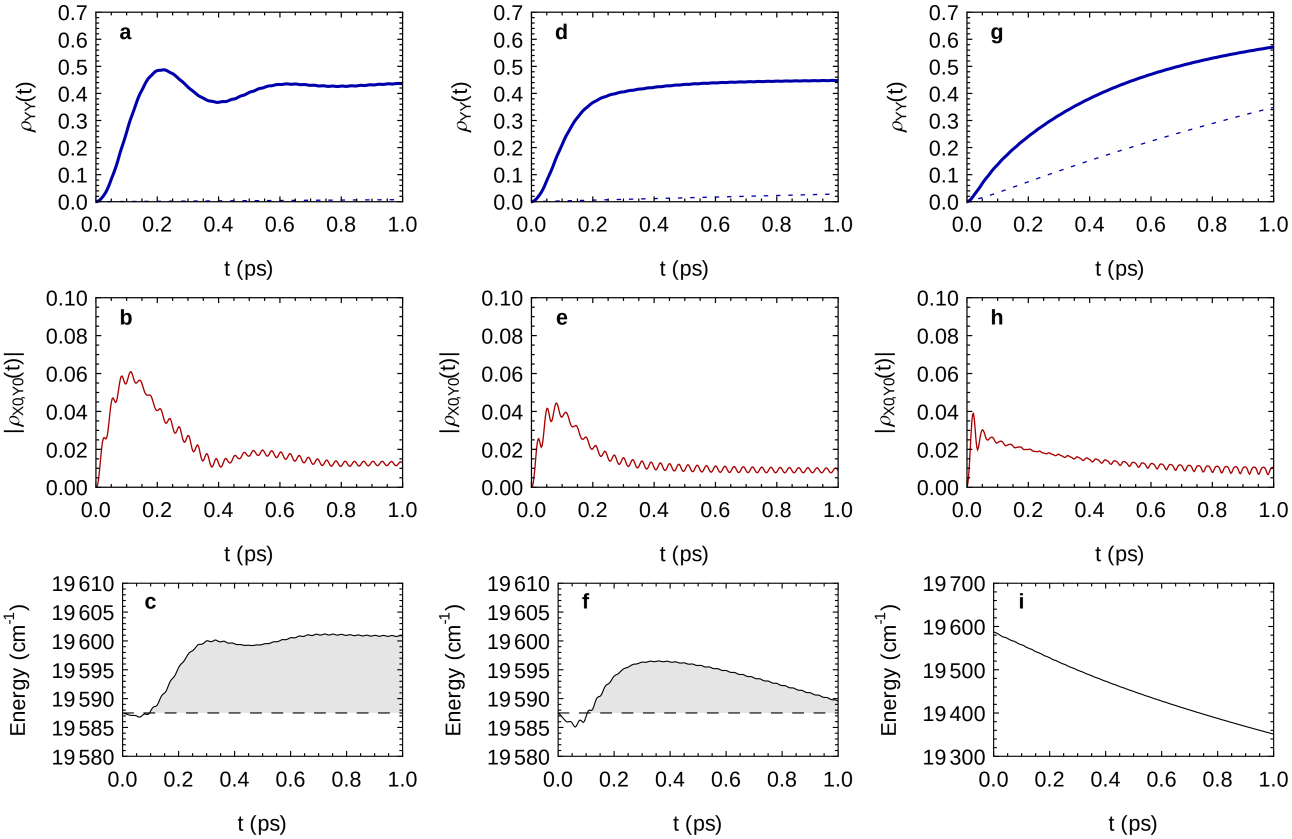

FIG. 2. The dynamics of $\rho_{YY}(t)$ (top row), $|\rho_{X0,Y0}(t)|$ (middle row) and Energy of the exciton vibration system (bottom row) for three interaction strengths to the low-energy thermal bath: **a-c**: $\lambda = 6\text{cm}^{-1}$, **d-f** $\lambda = 20\text{cm}^{-1}$ and **g-i**: $\lambda = 110\text{cm}^{-1}$

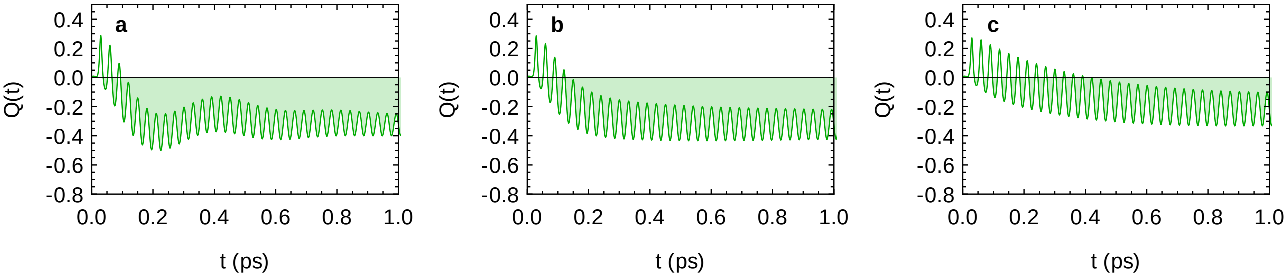

FIG. 3. **a-c** Dynamics of the Mandel Q-parameter for $\lambda = 6, 20, 110\text{cm}^{-1}$.

$r\,|X\rangle\langle X| - (1-r)\,|Y\rangle\langle Y|$ with $1/2 \le r \le 1$. The associated linear entropy quantifying the mixedness of the initial exciton states is given by $S_L = 2r(r-1)$. The time-averaged non-classicality (Figure 5 (a)) and average population transfer (Figure 5 (b)) follow similar decreasing monotonic trends for mixed states. These findings then suggest direct quantitative relationships between non-classicality and exciton population transport in the relevant time scale. *Outlook.-* Our work shows that in molecular dimers operating in the weak electronic coupling regime, exciton-vibrational resonances can trigger a non-classical response of a quasiresonant collective high-energy vibration thereby taking advantage of quantum fluctuations to efficiently populate a target exciton state. These non-classical fluctuations are observed for a variety of initial exciton conditions including statistical mixtures suggesting that such non-classicality may be triggered even under incoherent input of electronic population. These quantum phenomena could be experimentally accessible by transient coherent ultrafast phonon spectroscopy[42] which is sensitive to low-phonon populations of high-energy vibrations[43]. The framework here discussed could also be used to give more insight into the possible non-classical response of vibrational modes in other chemical sensors[44] which are conjectured to operate through weak electronic interactions[45]

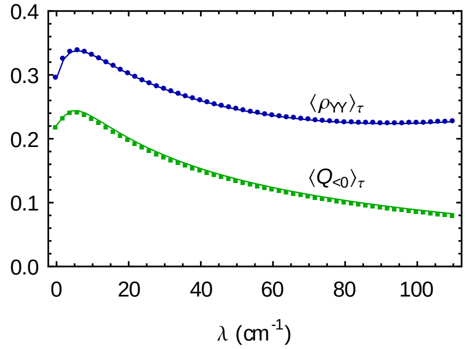

FIG. 4. Time integrated averages of exciton population $\rho_{YY}(t)$, inter-exciton coherent in the lowest vibrational level $|\rho_{X0-Y0}(t)|$ and non-classicality as quantified by $Q(t)\Theta[-Q(t)]$ (blue, red and green respectively) as functions of coupling to the thermal background by fixing environment cut-off frequency $\Omega_c = 100\text{cm}^{-1}$ and varying reorganization energy λ.

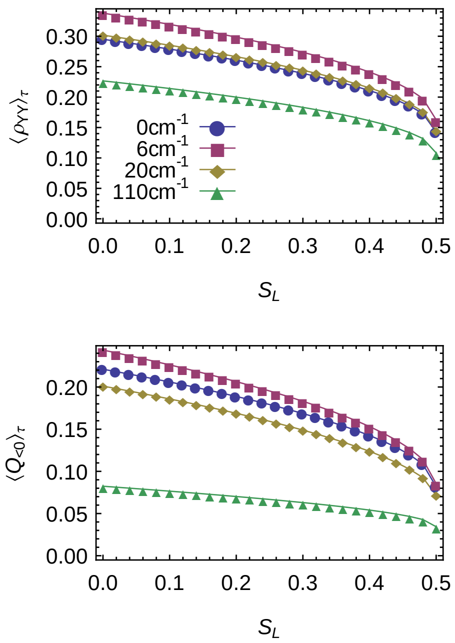

FIG. 5. The time integrated averages of exciton population $\rho_{YY}(t) - \rho_{YY}(0)$ and non-classicality as quantified by $Q(t)\Theta[-Q(t)]$ as functions of the linear entropy $S_L = 2r(r-1)$ for $0 < r < 1/2$. Curves are for different system-bath couplings.

to sense vibrational frequencies of the order of a thousand wavenumbers[46].

From a more general perspective, our work illustrates how exciton-vibrational resonances allow for rich dynamics of energy and coherences thereby providing a mechanism for adjusting the rates of entropy production and output energy. In this context, the associated vibrational dynamics could be understood as an internal quantum mechanism for thermodynamic control[47]. Understanding how quantum phenomena affect the thermodynamics of energy conversion in biomolecules could provide an unifying framework to quantify the advantages of quantum phenomena in a variety of biomolecular transport processes[48,49].

Acknowledgements.- We thank Greg Scholes and Rienk van Grondelle for discussions, and Avinash Kolli for support on numerical calculations in the initial stages of this project. Financial support from the Engineering and Physical Sciences Research Council (EPSRC UK) is gratefully acknowledged.

[1] Gregory S. Engel, Tessa R. Calhoun, Elizabeth L. Read, Tae-Kyu Ahn, Tomàš Mančal, Yuan-Chung Cheng, Robert E. Blankenship, and Graham R. Fleming. Evidence for wavelike energy transfer through quantum coherence in photosynthetic systems. *Nature*, 446(7137):782–786, Apr 12 2007.

[2] Gitt Panitchayangkoon, Dugan Hayes, Kelly A. Fransted, Justin R. Caram, Elad Harel, Jianzhong Wen, Robert E. Blankenship, and Gregory S. Engel. Long-lived quantum coherence in photosynthetic complexes at physiological temperature. *Proceedings of the National Academy of Sciences*, 107(29):12766–12770, 2010.

[3] Tessa R. Calhoun, Naomi S. Ginsberg, Gabriela S. Schlau-Cohen, Yuan-Chung Cheng, Matteo Ballottari, Roberto Bassi, and Graham R. Fleming. Quantum coherence enabled determination of the energy landscape in light-harvesting complex II. *The Journal of Physical Chemistry B*, 113(51):16291–16295, 2009.

[4] Elisabetta Collini, Cathy Y. Wong, Krystyna E. Wilk, Paul M. G. Curmi, Paul Brumer, and Gregory D. Scholes. Coherently wired light-harvesting in photosynthetic marine algae at ambient temperature. *Nature*, 463(7281):644–647, Feb 4 2010.

[5] Elad Harel and Gregory S. Engel. Quantum coherence spectroscopy reveals complex dynamics in bacterial light-harvesting complex 2 (LH2). *Proceedings of the National Academy of Sciences*, 2012.

[6] K. Birgitta Whaley, Mohan Sarovar, and Akihito Ishizaki. Quantum entanglement phenomena in photosynthetic light harvesting complexes. *Procedia Chemistry*, 3(1):152 – 164, 2011. 22nd Solvay Conference on Chemistry.

[7] M B Plenio and S F Huelga. Dephasing-assisted transport: quantum networks and biomolecules. *New Journal of Physics*, 10(11):113019, 2008.

[8] Patrick Rebentrost, Masoud Mohseni, Ivan Kassal, Seth Lloyd, and Aln Aspuru-Guzik. Environment-assisted quantum transport. *New Journal of Physics*, 11(3):033003, 2009.

[9] Thomas Renger, Volkhard May, and Oliver Kühn. Ultrafast excitation energy transfer dynamics in photosynthetic pigment-protein complexes. *Physics Reports*, 343(3):137–254, 2001.

[10] G. H. Richards, K. E. Wilk, P. M. G. Curmi, H. M. Quiney, and J. A. Davis. Coherent vibronic coupling in light-harvesting complexes from photosynthetic marine algae. *The Journal of Physical Chemistry Letters*, 3(2):272–277, 2012.

[11] Daniel B. Turner, Rayomond Dinshaw, Kyung-Koo Lee, Michael S. Belsley, Krystyna E. Wilk, Paul M. G. Curmi, and Gregory D. Scholes. Quantitative investigations of quantum coherence for a light-harvesting protein at conditions simulating photosynthesis. *Phys. Chem. Chem. Phys.*, 14:4857–4874, 2012.

[12] Jordan M. Womick and Andrew M. Moran. Vibronic enhancement of exciton sizes and energy transport in photosynthetic complexes. *The Journal of Physical Chemistry B*, 115(6):1347–1356, 2011.

[13] A. W. Chin, S. F. Huelga, and M. B. Plenio. Coherence and decoherence in biological systems: principles of noise-assisted transport and the origin of long-lived coherences. *Philosophical Transactions of the Royal Society A: Mathematical, Physical and Engineering Sciences*, 370(1972):3638–3657, 2012.

[14] A. W. Chin, J. Prior, R. Rosenbach, F. Caycedo-Soler, S. F. Huelga, and M. B. Plenio. The role of non-equilibrium vibrational structures in electronic coherence and recoherence in pigment-protein complexes. *Nature Physics*, 2013.

[15] Christoph Kreisbeck and Tobias Kramer. Long-lived electronic coherence in dissipative exciton dynamics of light-harvesting complexes. *The Journal of Physical Chemistry Letters*, 3(19):2828–2833, 2012.

[16] Avinash Kolli, Edward J. O'Reilly, Gregory D. Scholes, and Alexandra Olaya-Castro. The fundamental role of quantized vibrations in coherent light harvesting by cryptophyte algae. *Journal of Chemical Physics*, 137(17), Nov 7 2012.

[17] Niklas Christensson, Harald F. Kauffmann, Tõnu Pullerits, and Tomàš Mancǎl. Origin of long-lived coherences in light-harvesting complexes. *The Journal of Physical Chemistry B*, 116(25):7449–7454, 2012.

[18] Vivek Tiwari, William K. Peters, and David M. Jonas. Electronic resonance with anticorrelated pigment vibrations drives photosynthetic energy transfer outside the adiabatic framework. *Proceedings of the National Academy of Sciences*, 2012.

[19] Jason D. Biggs and Jeffrey A. Cina. Using wave-packet interferometry to monitor the external vibrational control of electronic excitation transfer. *The Journal of Chemical Physics*, 131(22):224101, 2009.

[20] Jason D. Biggs and Jeffrey A. Cina. Studies of impulsive vibrational influence on ultrafast electronic excitation transfer. *The Journal of Physical Chemistry A*, 116(7):1683–1693, 2012.

[21] Oliver Kühn, Thomas Renger, and Volkhard May. Theory of exciton-vibrational dynamics in molecular dimers. *Chemical Physics*, 204(1):99 – 114, 1996.

[22] Alexander B. Doust, Ivo H. M. van Stokkum, Delmar S. Larsen, Krystyna E. Wilk, Paul M. G. Curmi, Rienk van Grondelle, and Gregory D. Scholes. Mediation of ultrafast light-harvesting by a central dimer in phycoerythrin 545 studied by transient absorption and global analysis. *The Journal of Physical Chemistry B*, 109(29):14219–14226, 2005.

[23] Cathy Y. Wong, Richard M. Alvey, Daniel B. Turner, Krystyna E. Wilk, Donald A. Bryant, Paul M. G. Curmi, Robert J. Silbey, and Gregory D. Scholes. Electronic coherence lineshapes reveal hidden excitonic correlations in photosynthetic light harvesting. *Nature Chemistry*, 5(396-404), 2012.

[24] Th. Förster. 10th spiers memorial lecture. transfer mechanisms of electronic excitation. *Discuss. Faraday Soc.*, 27:7–17, 1959.

[25] Alejandro Perdomo, Leslie Vogt, Ali Najmaie, and Alàn Aspuru-Guzik. Engineering directed excitonic energy transfer. *Applied Physics Letters*, 96(9):093114, 2010.

[26] L. Mandel. Sub-poissonian photon statistics in resonance fluorescence. *Opt. Lett.*, 4(7):205–207, Jul 1979.

[27] D.N. Klyshko. Observable signs of nonclassical light. *Physics Letters A*, 213(1-2):7 – 15, 1996.

[28] Luiz Davidovich. Sub-poissonian processes in quantum optics. *Rev. Mod. Phys.*, 68:127–173, Jan 1996.

[29] M.O. Scully and S. Zubairy. *Quantum Optics*. Cambridge University Press, 1997.

[30] Alexander B. Doust, Christopher N.J. Marai, Stephen J. Harrop, Krystyna E. Wilk, Paul M.G. Curmi, and Gregory D. Scholes. Developing a structure-function model for the cryptophyte phycoerythrin 545 using ultrahigh resolution crystallography and ultrafast laser spectroscopy. *Journal of Molecular Biology*, 344(1):135 – 153, 2004.

[31] Vladimir I. Novoderezhkin, Alexander B. Doust, Carles Curutchet, Gregory D. Scholes, and Rienk van Grondelle. Excitation dynamics in phycoerythrin 545: Modeling of steady-state spectra and transient absorption with modified redfield theory. *Biophysical Journal*, 99(2):344 – 352, 2010.

[32] Hoda Hossein-Nejad, Alexandra Olaya-Castro, and Gregory D. Scholes. Phonon-mediated path-interference in electronic energy transfer. *The Journal of Chemical Physics*, 136(2):024112, 2012.

[33] Javier Prior, Alex W. Chin, Susana F. Huelga, and Martin B. Plenio. Efficient simulation of strong system-environment interactions. *Phys. Rev. Lett.*, 105:050404, Jul 2010.

[34] Yoshitaka Tanimura and Ryogo Kubo. Time evolution of a quantum system in contact with a nearly gaussian-markoffian noise bath. *Journal of the Physical Society of Japan*, 58(1):101–114, 1989.

[35] Akihito Ishizaki and Graham R. Fleming. Unified treatment of quantum coherent and incoherent hopping dynamics in electronic energy transfer: Reduced hierarchy equation approach. *The Journal of Chemical Physics*, 130(23):234111, 2009.

[36] Qiang Shi, Liping Chen, Guangjun Nan, Rui-Xue Xu, and YiJing Yan. Efficient hierarchical liouville space propagator to quantum dissipative dynamics. *The Journal of Chemical Physics*, 130(8):084105, 2009.

[37] G. Massimo Palma, Kalle-Antti Suominen, and Artur K. Ekert. Quantum computers and dissipation. *Proceedings: Mathematical, Physical and Engineering Sciences*, 452(1946):567–584, 1996.

[38] M Merlo, F Haupt, F Cavaliere, and M Sassetti. Sub-poissonian phononic population in a nanoelectromechanical system. *New Journal of Physics*, 10(2):023008, 2008.

[39] F Cavaliere, G Piovano, E Paladino, and M Sassetti. Phonon distributions of a single-bath mode coupled to a quantum dot. *New Journal of Physics*, 10(11):115004, 2008.

[40] Robert Silbey and Robert A. Harris. Variational calculation of the dynamics of a two level system interacting with a bath. *The Journal of Chemical Physics*, 80(6):2615–2617, 1984.

[41] Alessandro Zavatta, Valentina Parigi, and Marco Bellini. Experimental nonclassicality of single-photon-added thermal light states. *Phys. Rev. A*, 75:052106, May 2007.

[42] F. C. Waldermann, Benjamin J. Sussman, J. Nunn, V. O. Lorenz, K. C. Lee, K. Surmacz, K. H. Lee, D. Jaksch, I. A. Walmsley, P. Spizzirri, P. Olivero, and S. Prawer. Measuring phonon dephasing with ultrafast pulses using raman spectral interference. *Phys. Rev. B*, 78:155201, Oct 2008.

[43] K. C. Lee, M. R. Sprague, B. J. Sussman, J. Nunn, N. K. Langford, X.-M. Jin, T. Champion, P. Michelberger, K. F. Reim, D. England, D. Jaksch, and I. A. Walmsley. Entangling macroscopic diamonds at room temperature. *Science*, 334(6060):1253–1256, 2011.

[44] Luca Turin. A spectroscopic mechanism for primary olfactory reception. *Chemical Senses*, 21(6):773–791, 1996.

[45] Jennifer C. Brookes, Filio Hartoutsiou, A. P. Horsfield, and A. M. Stoneham. Could humans recognize odor by phonon assisted tunneling? *Phys. Rev. Lett.*, 98:038101, Jan 2007.

[46] Maria Isabel Franco, Luca Turin, Andreas Mershin, and Efthimios M. C. Skoulakis. Molecular vibration-sensing component in drosophila melanogaster olfaction. *Proceedings of the National Academy of Sciences*, 108(9):3797–3802, 2011.

[47] Noam Erez, Goren Gordon, Mathias Nest, and Gershon Kurizki. Thermodynamic control by frequent quantum measurements. *Nature*, 452(7188):724 – 727, 2008.

[48] Vladimir I. Novoderezhkin, Andrey G. Yakovlev, Rienk van Grondelle, and Vladimir A. Shuvalov. Coherent nuclear and electronic dynamics in primary charge separation in photosynthetic reaction centers: a redfield theory approach. *The Journal of Physical Chemistry B*, 108(22):7445–7457, 2004.

[49] Sam Hay and Nigel S. Scrutton. Good vibrations in enzyme-catalysed reactions. *Nature Chemistry*, 4(3):161–168, Mar 2012.

Appendix A: Hierarchical expansion of exciton-vibration dynamics

Here we provide details of the model for a system consisting of N electronic degrees of freedom each interacting with a quantized vibrational mode and the method used to accurately calculate the dynamics of these exciton-vibration systems. The system Hamiltonian $H_S = H_{\text{el}} \otimes \mathbb{1}_{\text{vib}} + \mathbb{1}_{\text{el}} \otimes H_{\text{vib}} + H_{\text{el-vib}}$, is defined by

$$H_{\text{el}} = \sum_{i=1}^{N} \varepsilon_i \sigma_i^+ \sigma_i^- + \sum_{i,j\leq i}^{N} V_{ij}(\sigma_i^+\sigma_j^- + \sigma_j^+\sigma_i^-) \tag{A1}$$

$$H_{\text{vib}} = \sum_{i=1}^{N} \omega_{\text{vib}}^i b_i^\dagger b_i \tag{A2}$$

and

$$H_{\text{el-vib}} = g_i \sigma_i^+ \sigma_i^- \otimes (b_i^\dagger + b_i) \ . \tag{A3}$$

Here, the operators $\sigma_i^{\pm}$ create/annihilate electronic excitations at site i, while $b_i^\dagger$ (b_i) create (annihilate) phonons associated with the vibrational mode of site i. ε_i denotes the excitation energies and V_{ij} the strength of interactions between sites. ω_{vib}^i is the frequency of the vibrational mode at site i and $g_i = \sqrt{S_i}\omega_{\text{vib}}^i$ the coupling of the mode to its site. S_i is the Huang-Rhys factor or mean number of phonons in the 'polaron cloud' formed when the mode is fully displaced. The the high energy modes considered here, we expand the quantized vibrational modes of the system in the basis of single phonon (Fock) states (*e.g.* $b_i = \sum_n^M (n+1)^{1/2} |n\rangle \langle n+1|$) truncating at M phonons. This system is then coupled to a continuum of bosonic modes (the thermal background) $H_B = \sum_{\mathbf{k}} \omega_{\mathbf{k}} b_{\mathbf{k}}^\dagger b_{\mathbf{k}}$, with an interaction

$$H_I = \sum_{\mathbf{k}} \sum_{i} g_{\mathbf{k},i}(\sigma_i^+\sigma_i^- \otimes \mathbb{1}_{\text{vib}})(b_{\mathbf{k}}^\dagger + b_{\mathbf{k}}) \ , \tag{A4}$$

such that a mode with frequency $\omega_{\mathbf{k}}$ is linearly coupled to the electronic excitation at site i with a strength $g_{\mathbf{k,i}}$ as specified by a spectral density $J_i(\omega) = \sum_{\mathbf{k}} |g_{\mathbf{k,i}}|^2 \delta(\omega - \omega_{\mathbf{k}})$. We assume the bath is spatially uncorrelated and identical for each site.

An infinite hierarchy of coupled differential equations[34–36] is used to express the dynamics of the exciton-vibration system density matrix $\rho_S(t)$. These read as,

$$\begin{aligned}
\partial_t \tilde{\rho}_{\boldsymbol{n}}(t) &= -i/\hbar[H_S, \tilde{\rho}_{\boldsymbol{n}}(t)] - \sum_{i=1}^{N}\sum_{k=0}^{K} n_{ik} v_{ik} \tilde{\rho}_{\boldsymbol{n}}(t) \\
&\quad -i \sum_{i=1}^{N} \left(\sum_{k=1}^{\infty} \frac{c_{ik}}{\nu_{ik}} - \sum_{k=1}^{K} \frac{c_{ik}}{\nu_{ik}} \right) [Q_i, [Q_i, \tilde{\rho}_{\boldsymbol{n}}(t)]] \\
&\quad - i \sum_{i=1}^{N}\sum_{k=0}^{K} \sqrt{(n_{ik}+1)|c_{ik}|} \left[Q_i, \ \tilde{\rho}_{\boldsymbol{n}_{ik}^+} \right] \\
&\quad - i \sum_{i=1}^{N}\sum_{k=0}^{K} \sqrt{n_{ik}/|c_{ik}|} \left(c_{ik}\, Q_i \tilde{\rho}_{\boldsymbol{n}_{ik}^-} - c_{ik}^*\, \tilde{\rho}_{\boldsymbol{n}_{ik}^-} Q_i \right) \ .
\end{aligned} \tag{A5}$$

for the case of a Drude spectral density and in a rescaled formulation[36] which admits their efficient adaptive timestep numerical integration. Operators $\tilde{\rho}_{\boldsymbol{n}}$ are indexed by the multi-index $\boldsymbol{n}$ which has entries n_{ik} and $n = \sum_{ik} n_{ik}$. $\boldsymbol{n}_{\boldsymbol{ik}}^{\pm}$ is $\boldsymbol{n}$ with entry $n_{jk} \to n_{jk} \pm 1$. The reduced density matrix of the system ρ_S is given by the operator $\tilde{\rho}_{\boldsymbol{0}}$. The coefficients ν_{ik} and c_{ik} are the Matsubara frequencies and coefficients appearing in the (truncated) exponential decomposition $\sum_{k=0}^{K} c_{ik} e^{-\nu_{ik} t}$ of the bath correlation function applied in Ref[35]. In the above terms $k > K$ are truncated with a Markovian approximation scheme[35]. This results in accurate dynamics for $K = 1$ at high temperatures ($\beta\Omega_c < 1$). In the present exciton-vibration case the system-bath coupling operator takes the form $Q_i = \sigma_i^+ \sigma_i^- \otimes \mathbb{1}_{\text{vib}}$.

Appendix B: B_0 parameter

Modulations of adjacent phonon number occupation as quantified by negative B_n, guarantees negative regions of a quasi-probability distribution[27] as is a potentially an experimentally accessible quantity. The non-classicality indicated by sub-Poissonian statistics is confirmed by negative $B_0 = 2P(0)P(2) - P(1)$. This arises from selective population of the $P(1)$ level of the relative displacement vibrational mode.

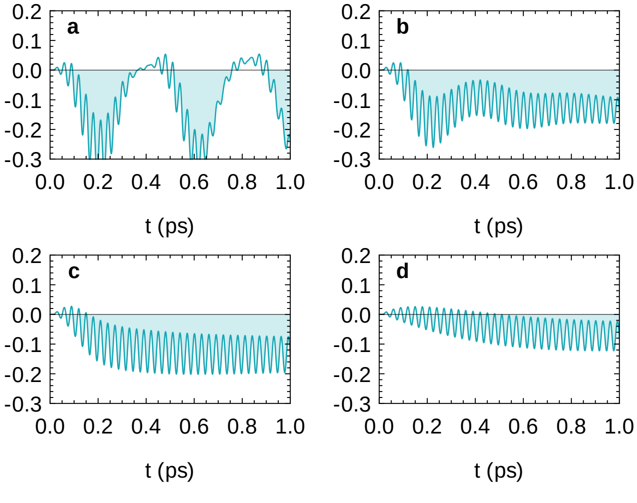

FIG. 6. B_0 for a) $\lambda = 0\text{cm}^{-1}$, b) $\lambda = 6\text{cm}^{-1}$, c) $\lambda = 20\text{cm}^{-1}$ and d) $\lambda = 110\text{cm}^{-1}$